

THE SPECTROSCOPIC ANALYSIS OF 2,4'-DIBROMOACETOPHENONE MOLECULE BY USING QUANTUM CHEMICAL CALCULATIONS

Etem KÖSE*

Department of Physics, Manisa Celal Bayar University, Manisa, Turkey

ABSTRACT

A spectroscopic investigation, used quantum chemical calculations, of 2,4'-dibromoacetophenone (2,4'-DBrA) molecule have been obtained in this paper. The calculations were supported the experimental results by IR, ¹H and ¹³C NMR techniques. Geometrical parameters and optimized energies of 2,4'-DBrA molecule were performed by density functional theory (DFT) B3LYP method 6-311++G(d,p) basis sets. After the geometry optimization of 2,4'-DBrA the vibrational spectra were obtained for this structure. The fundamental vibrations were assigned to base on potential energy distribution (PED) of the vibrational modes by using VEDA 4 (Vibrational Energy Distribution Analysis) program. Density of states for total (TDOS), partial (PDOS) and also overlap population (OPDOS) analysis were obtained. ¹H and ¹³C NMR chemical shifts were recorded by using the gauge-invariant atomic orbital (GIAO) method. Besides, electronic properties, such as HOMO and LUMO energies, were performed by time-dependent density functional theory (TD-DFT). Also, molecular electrostatic potential surface (MEPs) and thermodynamic properties were calculated for title molecule. The results are showed consistent with the obtained experimental results.

Keywords: 2,4'-dibromoacetophenone; DFT; FT-IR; NMR; MEPs

1. INTRODUCTION

Acetophenone and its derivatives have interesting biological, physicochemical and photochemical properties [1–3], also have very important pharmaceutical applications [4–10]. Acetophenone were exist in nature [11,12] and can be also acquired through the medium of various synthesis procedure [13,14]. The crystal structure of α -bromoacetophenone [15], 2-amino-5'-bromoacetophenone [16], ortho-hydroxy acetophenones derivatives [17], 4-hydroxy-3-(3-methyl-2-butenyl) acetophenone [18] were identified. There is seen in literature DFT studies of acetophenone and its derivatives such as; conformational analysis of acetophenone and α -substituted acetophenones were studied [19], the photodissociations of acetophenone was investigated [20], conformational stability of 4-hydroxy-3-methylacetophenone and 4-hydroxy-3-methoxyacetophenone and their vibrational spectra were analyzed [21], growth and characterization papers of 2-bromo-4-chloroacetophenone was published [22], structural and vibrational investigations of 5-fluro-2-hydroxyacetophenone was prepared [23], molecular properties and vibrational studies, and HOMO-LUMO energies of 3-bromoacetophenone were obtained by quantum chemical calculations [24], the detailed theoretical and experimental investigation (FT-IR and FT-Raman) of 3-aminoacetophenone [25], vibrational spectral investigation and, optimized parameters were computed for 4-chloro-2-bromoacetophenone [26], and 2,4-difluoroacetophenone molecule has a detailed spectroscopic studies [27,28].

*Corresponding Author: etemmm43@gmail.com

There is no similar studies about the 2,4'-DBrA molecule in the literature by utilized DFT calculations until now. So, an effort has been made about the geometrical, vibrational spectral evaluations, TDOS, PDOS, OPDOS analysis, ^{13}C and ^1H NMR chemical shifts calculations, electronic properties, molecular electrostatic potential surface (MEPs) and thermodynamic properties of 2,4'-DBrA were performed. The results are showed consistent with the obtained experimental results. This paper there will be important and considerable information before the synthesis new molecule and drug design and pharmaceutical applications.

2. THEORETICAL AND EXPERIMENTAL DETAILS

The infrared and (^1H and ^{13}C) NMR spectra of 2,4'-DBrA molecule were received from Spectral Database for Organic Compounds, SDBS as experimentally [29]. Theoretical calculations were done by utilized the Gaussian 09 program codes [30]. Geometric, vibration, and magnetic resonance analysis, atomic charges, dipole moment, thermodynamic properties, etc. were presented herein. The DFT [31] with the Becke's three-parameter hybrid functional (B3) [32,33] for the exchange part and the Lee–Yang–Parr (LYP) correlation function [34] was preferred, due to the a cost-effective approach its great accuracy in experimental values. The assignments of fundamental vibrational frequencies were made by VEDA program [35] according to their PEDs, and by Gauss view program [36] used visual animation. The time-dependent DFT (TD-DFT) method [37,38] with same basis set is utilized to calculate some electronic properties (UV–Vis spectra, excitation energies...). GIAO method [39,40] is one of the most common approach for nuclear magnetic shielding properties. Therefore, ^1H and ^{13}C NMR isotropic chemical calculations were obtained with the GIAO method based on optimized structure. The density of states (DOS) graphs; such as TDOS, PDOS and OPDOS of the studied molecule were prepared by using GaussSum 2.2 program [41]. The Mulliken atomic charges, MEPs, thermodynamic and NLO properties of 2,4'-DBrA molecule were given herein for the detailed physical and chemical information.

3. RESULTS AND DISCUSSION

Studied molecule has two substituent the first one COCH_2Br group and second Br (bromine) atom at para position. There is no seen an imaginary frequency at the C_s point group symmetry. Thence, the calculations were done based on the C_s symmetry group (see Table 1).

Table 1. The calculated energy and some thermodynamical parameters of 2,4'-DBrA at 298.15 K in ground state at the B3LYP/6-311++G(d,p) level

Parameters	C_s symmetry
Energy (Hartree)	-5532.079123290
Energy (kcal/mol)	-3471432.205
Zero point vib. energy (kcal mol $^{-1}$)	73.83045
Rotational constants (GHz)	3.16722
	0.14254
	0.13652
Specific heat, C_v (cal mol $^{-1}$ K $^{-1}$)	37.064
Entropy, S (cal mol $^{-1}$ K $^{-1}$)	108.338
Dipole moment (Debye)	3.3054
Imaginary frequencies	no

3.1. Potential Energy Surface (PES) Scan

The conformational analysis was done to see the most stable structure of the 2,4'-DBrA molecule. The torsion angles, between phenyl ring and COCH₂Br group, $\tau(\text{C}_{14}\text{-C}_{13}\text{-C}_3\text{-C}_4)$, changed every 10° (from 0° to 360°) by DFT/B3LYP method and 6-311++G(d,p) basis set. The obtained results indicate that there are three local minima near 0°, 180°, and 360° as seen Figure 1. The molecule was more stable for near these local (predicted as a global minima) minima. The optimized structures are controlled result of scan. The dihedral angles, $\tau(\text{C}_3\text{-C}_4\text{-C}_{13}\text{-C}_{14})$, $\tau(\text{C}_3\text{-C}_4\text{-C}_{13}\text{-O}_{12})$, $\tau(\text{Br}_{11}\text{-C}_1\text{-C}_6\text{-C}_5)$, and $\tau(\text{C}_4\text{-C}_{13}\text{-C}_{14}\text{-Br}_{17})$ etc. (predicted at 0°, and 180°, respectively) showed that the molecule has the C_s symmetry. All predictions of molecule for molecular structure, vibrational, NMR and electronic properties were obtained the most stable structure, chosen C_s point group symmetry.

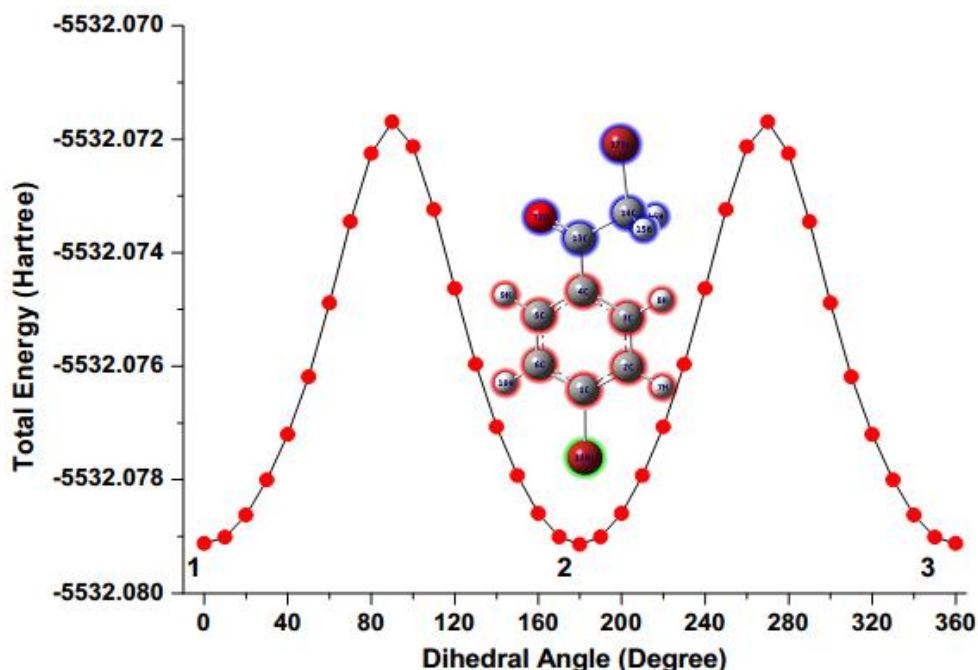


Figure 1. PES scan of selected degree T(H₁₂-N₁₀-C₁-C₂) of 2,4'-DBrA

3.2. Geometrical structures

The thermodynamical properties and energies of the headline molecule were given in Table 1 for C_s point group symmetry. The crystal structure of the 2,4'-DBrA has been not reached in the literature. For this reason, optimized geometric structural parameters were compared with the similar structure [15]. The optimized structure of the 2,4'-DBrA molecule was given as Figure 2 showing with the names and numbers of atoms. The results of optimized parameters of the studied molecule were listed in Table 2, based on the names and numbers of Figure 2.

The C-C bonds were predicted from 1.388 to 1.401 Å theoretically for present molecule. The experimental values were recorded from 1.373 to 1.429 Å, for α -bromoacetophenone (α -BA) molecule [15]. The C-C bonds were recorded from 1.375 to 1.398 Å for HF, from 1.389 to 1.412 Å for B3LYP and 1.384 to 1.403 Å for LSDA [28]. For 2,4-difluoroacetophenone, these bonds were predicted from 1.375 to 1.398 Å by using B3LYP method 6-311++G(d,p) basis set [27]. There are seen little differences angles slightly out of perfect hexagonal structure in the phenyl ring. It is due to the substitutions of the bromine atom, oxygen atom and CH₂Br groups in the place of H atoms (see Table 2). The results of C-C bonds lengths are very good correlated with the literature [6,7,15,18,21,25-28] for the structurally similar molecules.

The halogens F, Cl, Br... have a role in the molecule as substituent in place of hydrogen atom these bond lengths (C-X) show a remarkable increment. The C-Br bond lengths were predicted 1.912 Å (for C-Br₁₁) and 1.951 Å (for C-Br₁₇), by using DFT/B3LYP method with 6-311++G(d,p) basis set. The bond C-Br₁₇ were observed at 1.929 Å for α -bromoacetophenone molecule [15]. The C-Br bond lengths show small differences in literature [15] according to location of halogen Br atoms in present molecule. The C-Br bond were predicted 1.917 Å for 5-bromosalicylic acid [42] 1.921 Å for 3-bromophenylboronic acid [43] 1.922 Å and 1.920 Å 2/6-bromonicotinic acid molecules [44]. These bonds (at the para position) are very closely in literature (above), due to the similar structures.

There are seen some deviation both endohedral and exohedral angles; such as the angles of C-C-C and C-C-H bonds were differed from normal value of ring angle 120.0°. These deviations can be caused by the substitutions, Br atoms and COCH₂Br group. The dihedral angles were predicted τ (C₃-C₄-C₁₃-C₁₄) as 0.0°, τ (C₃-C₄-C₁₃-O₁₂) as 180.0°, and τ (Br₁₁-C₁-C₆-C₅) as 180.0° for studied molecule. These state show that stable structure must be planer and C_s symmetry group symmetry. Reminding as; the theoretical results belong to vapor phase, there have been some acceptable differences from the experimental results.

Table 2. The experimental for α -bromoacetophenone (α -BA) and optimized bond lengths (Å) and angles (°) molecule for 2,4'-DBrA molecule by using B3LYP/6-311++G(d,p) method

Parameters	Exp. ^a	2,4'-DBrA	Parameters	Exp. ^a	2,4'-DBrA
Bond Lengths (Å)	α -BA		Bond Angles (°)	α -BA	
C ₁ -C ₂	1.373	1.392	C ₃ -C ₄ -C ₁₃	119.2	123.5
C ₁ -C ₆	1.397	1.394	C ₅ -C ₄ -C ₁₃	125.6	117.7
C ₁ -Br ₁₁		1.912	C ₄ -C ₅ -C ₆	122.7	121.0
C ₂ -C ₃	1.401	1.392	C ₄ -C ₅ -H ₉	-	118.5
C ₂ -H ₇	-	1.082	C ₆ -C ₅ -H ₉	-	120.5
C ₃ -C ₄	1.429	1.401	C ₁ -C ₆ -C ₅	116.4	119.1
C ₃ -H ₈	-	1.083	C ₁ -C ₆ -H ₁₀	-	120.3
C ₄ -C ₅	1.391	1.402	C ₅ -C ₆ -H ₁₀	-	120.6
C ₄ -C ₁₃	1.486	1.502	C ₄ -C ₁₃ -O ₁₂	122.5	121.2
C ₅ -C ₆	1.393	1.388	C ₄ -C ₁₃ -C ₁₄	119.5	116.4
C ₅ -H ₉	-	1.083	O ₁₂ -C ₁₃ -C ₁₄	117.5	122.4
C ₆ -H ₁₀	-	1.082	C ₁₃ -C ₁₄ -H ₁₅	-	110.4
O ₁₂ -C ₁₃	1.258	1.209	C ₁₃ -C ₁₄ -H ₁₆	-	110.4
C ₁₃ -C ₁₄	1.552	1.529	C ₁₃ -C ₁₄ -Br ₁₇	111.5	113.6
C ₁₄ -H ₁₅	-	1.090	H ₁₅ -C ₁₄ -H ₁₆	-	108.7
C ₁₄ -H ₁₆	-	1.090	H ₁₅ -C ₁₄ -Br ₁₇	-	106.8
C ₁₄ -Br ₁₇	1.929	1.951	H ₁₆ -C ₁₄ -Br ₁₇	-	106.8
Bond Angles (°)			Selected Dihedral Angles (°)		
C ₂ -C ₁ -C ₆	122.8	121.3	C ₃ -C ₄ -C ₁₃ -O ₁₂	-	180.0
C ₂ -C ₁ -Br ₁₁	-	119.3	C ₃ -C ₄ -C ₁₃ -C ₁₄	-	0.0
C ₆ -C ₁ -Br ₁₁	-	119.4	Br ₁₁ -C ₁ -C ₆ -C ₅	-	180.0
C ₁ -C ₂ -C ₃	118.0	119.1	Br ₁₁ -C ₁ -C ₂ -C ₃	-	180.0
C ₁ -C ₂ -H ₇	-	120.4	C ₄ -C ₁₃ -C ₁₄ -H ₁₅	-	-60.1
C ₃ -C ₂ -H ₇	-	120.5	C ₄ -C ₁₃ -C ₁₄ -H ₁₆	-	60.1
C ₂ -C ₃ -C ₄	120.7	120.9	C ₄ -C ₁₃ -C ₁₄ -Br ₁₇	-	180.0
C ₂ -C ₃ -H ₈	-	118.2	O ₁₂ -C ₁₃ -C ₁₄ -H ₁₅	-	119.9
C ₄ -C ₃ -H ₈	-	121.0	O ₁₂ -C ₁₃ -C ₁₄ -H ₁₆	-	-119.9
C ₃ -C ₄ -C ₅	120.2	118.8	O ₁₂ -C ₁₃ -C ₁₄ -Br ₁₇	-	0.0

^aThe X-Ray data from ref. [15]

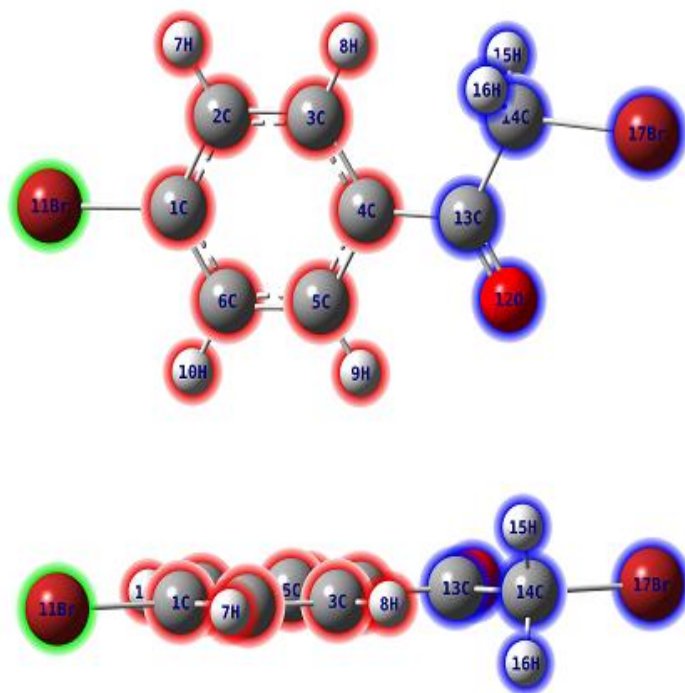


Figure 2. The theoretical optimized geometric structures of the 2,4'-DBrA molecule

3.3. Vibrational Spectral Analysis

The analyses of vibrational spectra were done to provide helpful and realistic accommodation. Theoretical section were utilized by DFT/B3LYP method, 6-311++G(d,p) basis set. The theory was carried out in vacuum, while experimental ones for solid phase, for this reason some differences were seen. The theoretical results were multiplied by scaling factor [32] to get suitable with the experimental results. Theoretical (IR and Raman) vibrational spectra (with scaling factor) were presented in Figure 3 and experimental IR spectrum was given in Figure 4.

The molecule has 17 atoms and 45 ($3N-6$) fundamental modes in the C_s symmetry. The fundamental vibrational modes were divided as A'' representing out of plane and A' representing in-plane motions ($30A' + 15A''$). The results of vibrational frequencies both theoretical and experimental (IR), with their assignments were collected in Table 3.

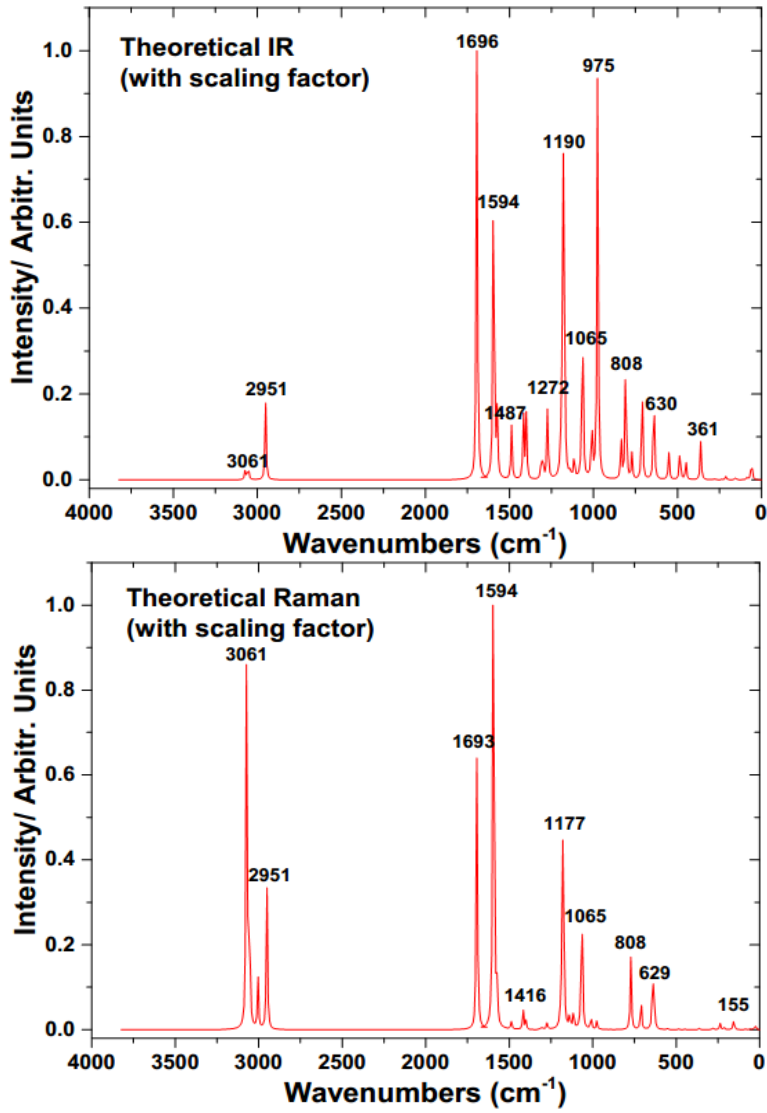


Figure 3. The calculated FT-IR and FT-Raman spectra of (with the scale factor) 2,4'-DBrA

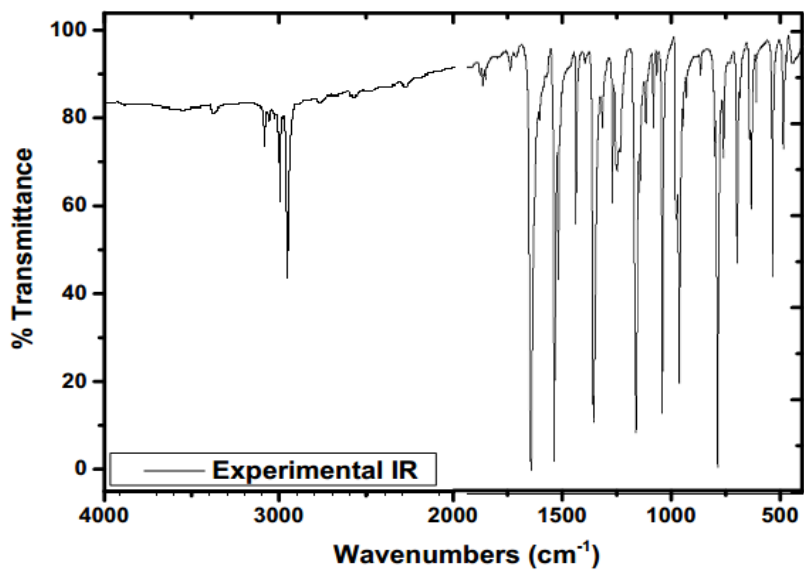


Figure 4. The experimental IR spectra of 2,4'-DBrA

Table 3. Comparison of the calculated harmonic frequencies and experimental (IR) wavenumbers (cm^{-1}) using by B3LYP method 6-311++G(d,p) basis set of 2,4'-DBrA molecule

Mod e No	Sym. Specie s	Theoretical		Exp. FT-IR	Assignments PED ^b ($\geq 10\%$)
		Unscaled freq.	Scaled freq. ^a		
v ₁	A'	3208	3073	3084	vCHring _{sym.} (100)
v ₂	A'	3206	3071	3059	vCHring _{sym.} (100)
v ₃	A'	3195	3061		vCHring _{asym} (99)
v ₄	A'	3187	3053		vCHring _{asym} (100)
v ₅	A''	3136	3004	3000	vCH _{2asym} (100)
v ₆	A'	3080	2951	2951	vCH _{2sym} (100)
v ₇	A'	1767	1693	1692	vC=O (90)
v ₈	A'	1621	1594	1588	vCC (62), i.p. CH[δ CCH (19), δ CCC (18)] δ
v ₉	A'	1600	1572	1567	vCC (61), i.p. CH[δ CCH (26), δ CCC (10)]
v ₁₀	A'	1513	1487	1484	i.p. CH [δ CCH (63), δ CCC (19)], vCC (15)
v ₁₁	A'	1441	1416		ρ CH ₂ (88)
v ₁₂	A'	1423	1399	1397	vCC (42), i.p. CH[δ CCH (41), δ CCC (11)]
v ₁₃	A'	1332	1309	1309	i.p. CH[δ CCH (62)], vCC (27)
v ₁₄	A'	1321	1298	1292	ring def. [vCC (70)], i.p. CH [δ CCH (24)]
v ₁₅	A'	1294	1272	1272	γ CH [τ CCCH (53), vCC (25)]
v ₁₆	A'	1211	1190	1198	i.p. CH [δ CCH (43), vCC (35)]
v ₁₇	A'	1197	1177	1177	i.p. CH + δ CH ₂ [δ CCH (45), δ CCC (11)], vCC (29)
v ₁₈	A''	1157	1138	1161	ϕ CH ₂ [δ CCBr (80), τ CCCH (11)]
v ₁₉	A'	1133	1114	1114	i.p. CH [δ CCH (54)], vCC (35)
v ₂₀	A'	1083	1065	1072	vCC (67), δ CCH (15), vCBr (12)
v ₂₁	A'	1027	1010	1005	ring def. [δ CCC (78), vCC (11)]
v ₂₂	A''	1004	987	991	γ CH [τ CCCH (85), τ CCCC (14)]
v ₂₃	A'	992	975	973	vCC (48), ω CH ₂ [δ CCC (25), δ CCO (16)]
v ₂₄	A''	971	954		γ CH [τ CCCH (78), τ CCCC (15)]
v ₂₅	A''	908	892		γ CH [τ CCCH (57)], Γ CH ₂ [τ CCCCO (24), τ CCCC (10)]
v ₂₆	A''	850	835	823	γ CH [τ CCCH (94)]
v ₂₇	A''	822	808	808	γ CH [τ CCCH (76), τ CCCC (13)]
v ₂₈	A'	785	771	781	ring breath. vCC (47), δ CCC (30)
v ₂₉	A'	722	710	717	vCBr (27), δ CCC (30), δ CCO (15), δ CCBr (14)
v ₃₀	A''	719	707		γ CH [τ CCCC (72), τ CCCH (16)]
v ₃₁	A'	651	640	649	vCBr (45), δ CCO(12), ring breath. δ CCC (28), vCC (10)]
v ₃₂	A'	640	629		ring def.[δ CCC (75), vCC (12)]
v ₃₃	A''	561	552	546	ϕ CH ₂ [τ CCCCO(28), τ CCCBBr (21)], τ CCCH (17), τ CCCC (27)
v ₃₄	A'	493	485	497	vCC (38), δ CCC (26), vCBr (17), δ CCO (14)
v ₃₅	A''	457	450		ϕ CH ₂ [τ CCCBBr (31) τ CCCCO (17)], τ CCCC (26), τ CCCH (23)
v ₃₆	A''	412	405		γ CH [τ CCCC (86), τ CCCH (14)]
v ₃₇	A'	367	361		δ CCC (40),vCBr (32), δ CCBr (12)
v ₃₈	A'	284	279		δ CCC (37),vCBr (24), δ CCBr (27)
v ₃₉	A''	241	237		τ CCCC (49), τ CCCBBr (35), τ CCCCO (12)
v ₄₀	A'	216	212		horse riding [vCBr (61), δ CCC (17), δ CCO (11)]
v ₄₁	A'	158	155		vCC (22), δ CCC (18), vCBr (25), δ CCBr (34)
v ₄₂	A'	87	85		δ CCC (62), δ CCBr (28)
v ₄₃	A''	85	84		Γ CH ₂ [τ CCCC (48), τ CCCBBr (34)], τ CCCH (11)
v ₄₄	A''	60	59		Γ CH ₂ [τ CCCC(74), τ CCCBBr (17)]
v ₄₅	A''	27	27		τ CCCC (61) τ CCCBBr (36)

^aWavenumbers in the ranges from 4000 to 1700 cm^{-1} and lower than 1700 cm^{-1} are scaled with 0.958 and 0.983 for B3LYP/6-311++G(d,p) basis set, respectively.

^bPED: Potential Energy Distribution ν ; stretching, γ ; out-of plane bending, δ ; in-plane-bending, τ ; torsion, ρ ; scissoring, ω ; wagging, ϕ ; twisting, Γ ; rocking.

3.3.1. Stretching modes

C–H stretching vibrations were come in view characteristic region between 3000 and 3100 cm^{-1} . Similar molecules, having the C–H stretching in literature [21–27], modes, show multiple peaks in range of ca. 3000–3100 cm^{-1} for aromatic ring. The C–H stretching modes were also seen the methyl group (CH_3) was shaped as methylene (CH_2) since one of the H atom replaced by Br atom. These modes were normally falling that in the region 2840–3000 cm^{-1} [26,45,46], for the molecules include aromatic methyl compounds. Both phenyl ring and methylene (CH_2) group have symmetric and asymmetric modes of C–H stretching vibrations. The symmetric C–H modes appeared higher frequencies than asymmetric ones in the phenyl ring, however there is seen opposite situation in the methylene group. In this study, the C–H stretching modes were predicted in the region 3053–3073 cm^{-1} (3059–3084 cm^{-1} IR) for phenyl ring and 2951–3003 cm^{-1} (2951–3003 cm^{-1} IR) for methylene group. According to PED this vibrations are a pure mode as evident from the contribution of $\sim 100\%$.

One of the most popular, very important and characteristic, modes are C–C stretching vibrations in aromatic rings. Especially, Varsányi's study [47] is given as a reference for this mode, seen at 1625–1590, 1590–1575, 1540–1470, 1465–1430 and 1380–1280 cm^{-1} from the frequency ranges for the five bands. The stretching vibrations were predicted in the region of 1594–1487, 1399–1177, 1114–1010, 975, 771, 640, 629, 485, and 155 cm^{-1} in this study. The highest contributions come from modes ν_{14} , ν_{20} , as percentages 70% and 67%, respectively. The other important contributions were seen modes of ν_8 , ν_9 , contributed over sixty percent. The C–C modes were combined with C–H in-plane bending and assigned ring deformation modes. The theory falls in to their experimental results, showing good agreement. There is also seen concordance with the similar structure in the literature [21–27].

C–Br stretching modes were seen at the region of 200–480 cm^{-1} in bromine compounds by Varsányi [47]. According to PED and GaussView results, the C–Br modes are no pure vibrations, mixed other vibrations. These modes were predicted at 155, 212, 279, 361, 485, 640, 710, 1065 cm^{-1} , respectively. The mode C–Br stretching (para position) occurred by Mooney [48], the mode of the C–Br were recorded at 308 cm^{-1} in FT-Raman and theoretically calculated at 292 cm^{-1} [43], 358 cm^{-1} in FT-Raman spectrum and calculated theoretically 396 and 233 cm^{-1} by using B3LYP/6-311G(d,p) basis set [49]. These vibrations were observed as a medium FT-IR band at 532 cm^{-1} , predicted at 573 cm^{-1} for *p*-bromophenoxyacetic acid [50], and calculated at 547 and 389 cm^{-1} for 4-bromophenylboronic acid [51]. So, there is no big difference between these studies.

The C=O stretching modes are also showing a characteristic properties in the vibrations modes of carbonyl groups. The stretching modes of carbonyl in ketones are expected in the region nearly 1700 cm^{-1} [46,52,53]. In this study, theoretically strong and medium bands were occurred for IR and Raman spectra and predicted at 1693 cm^{-1} . The experimental IR spectrum has also strong band at 1692 cm^{-1} . In literature, the C=O stretching modes were observed, very strong band at 1690 cm^{-1} in FT-IR and FT-Raman spectra [26], very strong band, at 1668 cm^{-1} in FT-IR and at 1665 cm^{-1} in FT-Raman, predicted 1746 cm^{-1} [25], very strong band at 1692 cm^{-1} in FT-Raman and calculated at 1685, 1690 and 1649 cm^{-1} at HF/6-31G, B3LYP/6-31G and LSDA/6-31G levels of theory, respectively [28]. The modes of C=O stretching vibrations were showed very good agree terms of intensity and frequency.

3.3.2. Bending and deformation modes

The bending modes are separated generally as in plane bending (i.p.) and out-of-plane (o.o.p.) bending C–H vibrations modes appear in the range of 1000–1300 cm^{-1} and at 750–1000 cm^{-1} , respectively [53,54]. The i.p. C–H bending modes were calculated at 1487–1594, 1298–1399, 1177–1190, and 1114 cm^{-1} and observed 1484–1588, 1292–1397, 1177–1198, and 1114 cm^{-1} in FT-IR, in this paper. Generally these modes are mixed or combined the other ring modes, especially CCC modes. The o.o.p. C–H bending modes are (assigned ν_{15} , ν_{22} , ν_{24-27} , ν_{30} , and ν_{36}) predicted at 1272, 987, 954–808, 707, and 405 cm^{-1} , respectively. The experimental values were seen at 1272, 991, and 823–808 cm^{-1} , respectively. Both i.p. and o.o.p. C–H bending modes were determined simulation of GaussView program. These results and their PED showed that highly pure modes. In literature, similar structure molecules were supported [21–27] and good agree for obtained data.

For the group $-\text{CH}_2-\text{CO}-$, the methylene scissoring vibration occurs in the range $1435\text{--}1405\text{ cm}^{-1}$ [55]. Also, in the present work, the scissoring modes of CH_2 was obtained 1416 cm^{-1} showing good agree. The CH_2 twisting and wagging vibrations were recorded at $450, 552, 1138\text{ cm}^{-1}$ and at 975 cm^{-1} , respectively. The C–Br bending modes both i.p. and o.o.p. appear in variable region based on the state of the bromine substituent of structure. The i.p. C–Br modes were calculated at $85, 155, 279, 361$ and 710 cm^{-1} which assigned to only at 717 cm^{-1} in FT-IR. The o.o.p. C–Br bending modes were calculated at $27, 237\text{ cm}^{-1}$ and (450 and $552, \text{ cm}^{-1}$, assigned ϕCH_2 with CCCO torsion mode), observed 546 cm^{-1} in the FT-IR. The other bending and torsion modes of the related bromine atom accounted in Table 3. The CCC i.p. bending modes were contaminated the other modes, and seen in the large region. The largest one i.p. bending modes of CCC were calculated at 1010 and 629 cm^{-1} , assigned as ring deformation modes and observed (FT-IR) at 1005 cm^{-1} .

There is only FT-IR experimental data in this paper. Between the calculated and experimental wavenumbers has very good correlation. To see the correlation clearly Figure 5 graphic were plotted. The description of this correlation was given as equation as linear following;

$$\nu_{\text{exp}} (\text{cm}^{-1}) = 1.0039 \nu_{\text{cal}} - 6.0428 \quad (\text{R}^2 = 0.9999) \quad \text{for IR spectra}$$

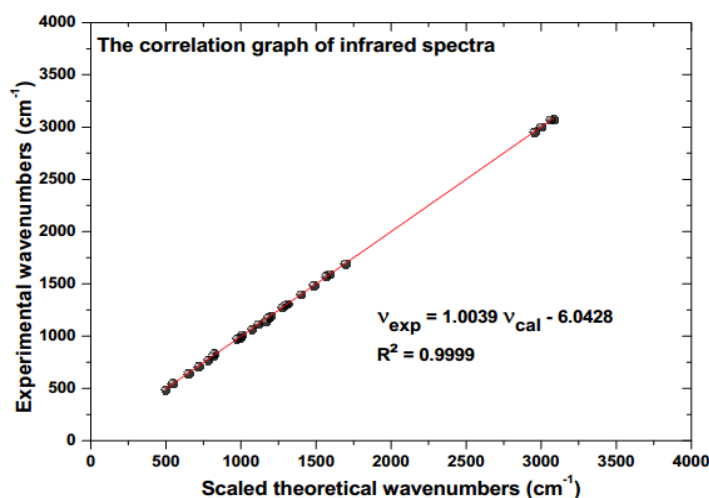


Figure 5. The correlation graphic of theoretical and experimental FT-IR spectra of 2,4'-DBrA

3.4. NMR Spectrum Analysis

^1H and ^{13}C NMR spectra were obtained [29] and predicted due to providing detailed information. Firstly, full geometry optimization were done and, using the gauge-including atomic orbital (GIAO) [39,40] approach with the DFT/B3LYP method, and 6-311++G(d,p) basis set for chemical shifts predictions. NMR spectra are important to obtain chemical, physical, and structural information about the molecules. NMR spectra and its computer simulation methods give an efficient way to predict and interpret structure of molecules [56]. So, the experimental and theoretical ^1H and ^{13}C NMR investigations were investigated, in this section. The experimental (in CDCl_3) ^1H and ^{13}C NMR spectra were presented in Figure 6a-6b, respectively. The results of experimental and calculated NMR spectra were gathered in Table 4 according to atom positions of Figure 2.

There is a seen two type hydrogen atom of the studied molecule as in CH_2 groups and phenyl ring. The chemical shifts of protons (ring) generally are seen in the range of $7.00\text{--}8.00\text{ ppm}$ for organic molecules. The chemical shifts of ring for this study were predicted at $7.70\text{--}8.47\text{ ppm}$ (CDCl_3), $7.55\text{--}8.48\text{ ppm}$ (gas), and $7.76\text{--}8.44\text{ ppm}$ (DMSO). The experimental results were recorded at $7.64\text{--}7.84\text{ ppm}$ (CDCl_3). The CH_2 groups' protons were resonance at 4.39 and 4.96 ppm (CDCl_3) and 4.70 ppm

(gas), 5.09 ppm (DMSO). The electronic environments are very important for the variation of chemical shifts. The electron-withdrawing and -donating in the atoms or atom groups, (attached or nearby of hydrogen), can reduced the shielding and move the resonance of their protons to a higher frequency and lower frequency, respectively [57]. The CH₂ protons have electron-withdrawing environments, so the shielding and resonance decreased. The protons generally can be more susceptible to intermolecular interactions than the other heavier atoms [58]. So, the solvent effect to these proton signals. The theoretical values were parallel nearly same region, showed well agree.

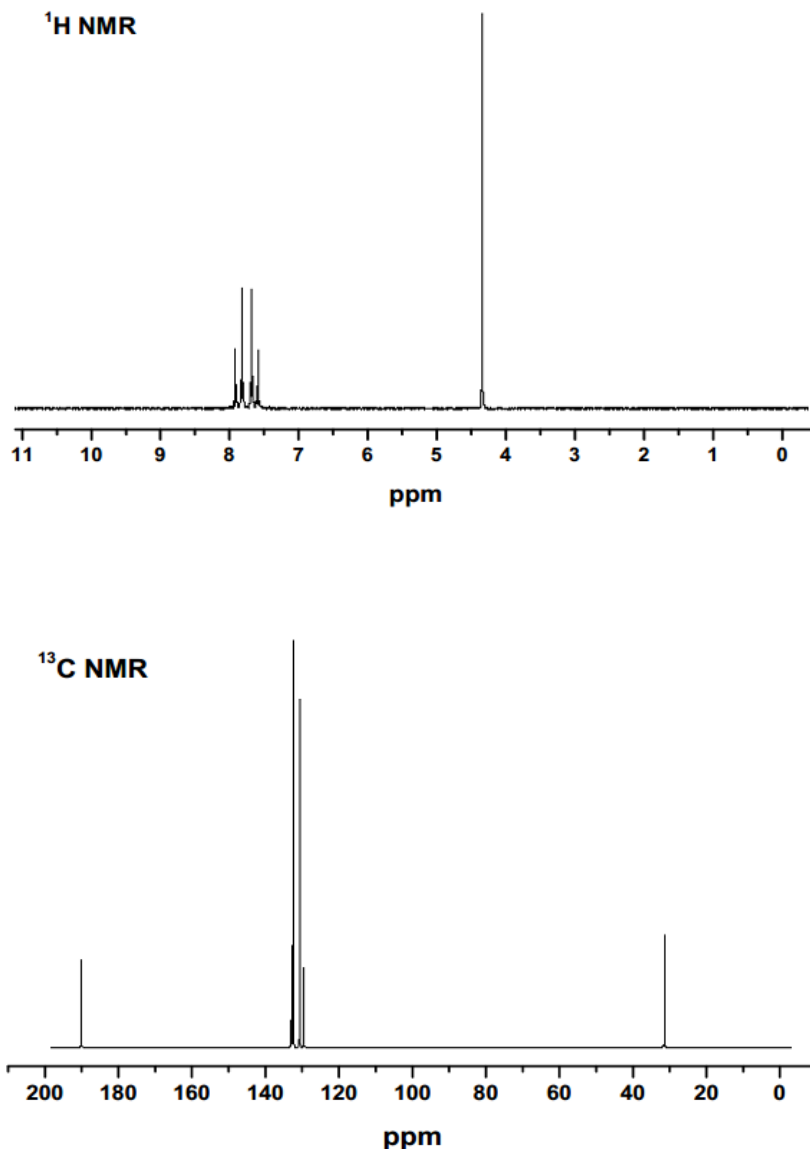


Figure 6. (a) ¹H NMR (b) ¹³C NMR spectra of 2,4'-DBrA molecule in CDCl₃ solution

Table 4. The experimental and theoretical, ^1H and ^{13}C NMR isotropic chemical shifts (with respect to TMS) of 2,4'-DBrA molecule with DFT (B3LYP 6-311++G(d,p)) method

Atoms	Exp.	Theoretical	
	CDCl_3	CDCl_3	Gas
C(1)	129.30	155.10	155.08
C(6)	132.20	137.61	137.67
C(2)		136.68	135.94
C(3)	130.40	134.22	132.54
C(5)		135.21	135.59
C(4)	132.70	137.87	137.83
C(13)	190.40	194.57	191.71
C(14)	30.40	53.94	52.38
H(8)	7.84	7.83	7.60
H(9)		8.47	8.48
H(7)	7.64	7.70	7.55
H(10)		7.78	7.69
H(15)	4.39	4.96	4.70
H(16)			

The carbons' chemical shifts can be evaluated two-stage as ring and others for this paper. Generally, the chemical shifts of carbons (ring) are recorded and overlapped region between 100 to 150 ppm [59,60]. Both aldehydes and ketones have a characteristic carbon of carbonyl group ($\text{C}=\text{O}$) at 190–215 ppm and methyl groups at nearly 30 ppm [61]. The present case, ring carbon chemical shifts predicted at 134.22–155.10 (CDCl_3) in theoretically and observed 129.30–132.70 in experimentally. There are seen important differences between the theory and experiment for the C(1) and C(14) atoms. It can be that the theoretical calculations taken into account very sensitive the bromine atoms effects. The chemical shifts of carbon [C(2), C(6)] and [C(3), C(5)] atoms nearly the same due to the similar environments. The carbon atom of carbonyl group, C(13), of this study were resonance at 190.40 ppm (experiment) 194.57 ppm (theory) in the CDCl_3 solvent. The C(1) atom shifts were also predicted at 155.10 ppm bigger than other ring carbons, due to the highly electronegative properties of bromine atom. There is seen similar state in literature [27], supported our experimental and theoretical results.

Between the experimental and theoretical results of NMR chemical shifts are showing good correlations. The graphic in Figure 7 and following equation were presented very clearly this correlation.

$$\delta_{\text{cal.}} (\text{ppm}) = 1.0331 \delta_{\text{exp.}} + 3.1894 \quad (R^2 = 0.9876)$$

As results, the theoretical ^1H and ^{13}C chemical shifts data show well agree the experiment. However, very small differences can be solvent effects, and local magnetic field effect.

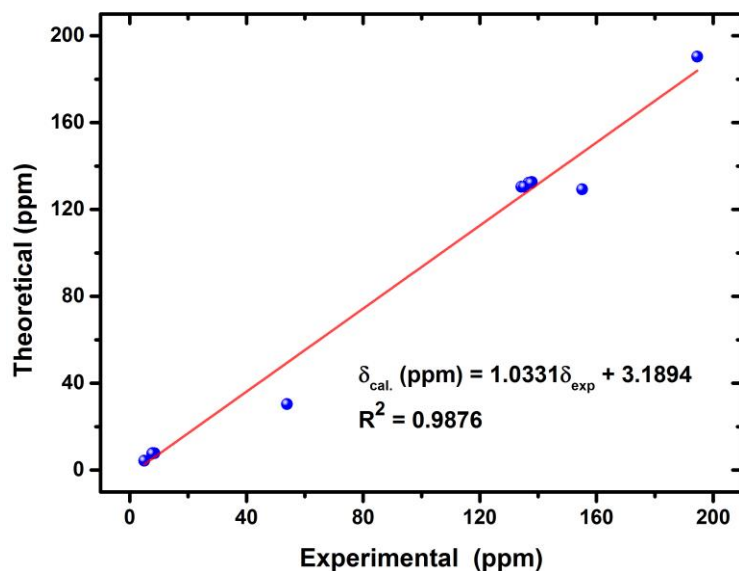


Figure 7. Correlation graphic of NMR spectra of the 2,4'-DBrA molecule in CDCl_3 solution

3.5. Electronic Characteristics Details

3.5.1. UV-Vis spectrum and molecular orbital investigations

Electronic properties and molecular orbital investigations were investigated by TD-DFT method. It present a fairly good reasonable results for medium size molecules [37,38]. In the absence of experimental results to shed light on literature and to support future studies, The theoretical UV-Vis (electronic absorption) spectra and molecular orbital analysis were prepared by using TD-DFT method B3LYP/6-311++G(d,p) basis set ($n=12$ state and root=40). The obtained theoretical UV-Vis (electronic absorption) spectra of title molecule were given for gas phase, ethanol, and water solvent in Figure 8. For the gas phase, ethanol and water solvent; the calculated absorption (λ), excitation energies (E), oscillator strength (f), and counterparts with major contributions by GaussSum 2.2 [41] program, were gathered in Table 5. The maximum wavelengths were recorded at about 272-275 nm for all solvents.

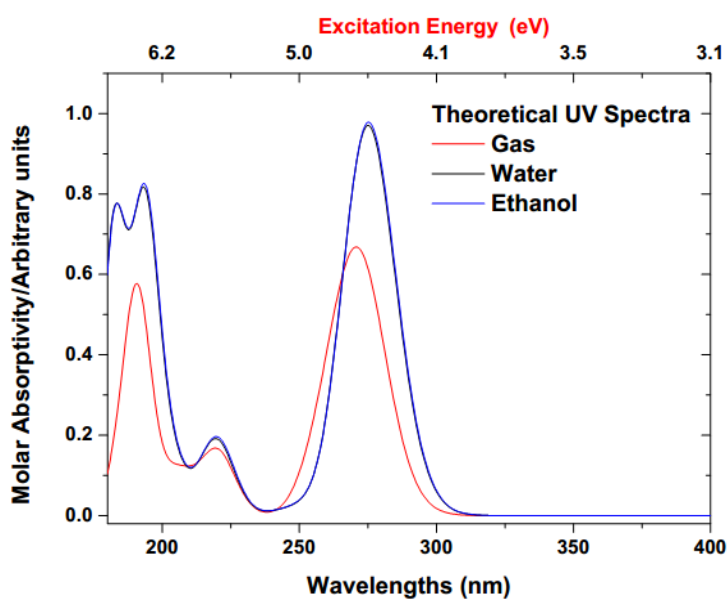


Figure 8. The theoretical UV-Vis spectra of 2,4'-DBrA molecule gas phase, in ethanol and water

Table 5. The calculated absorption wavelengths λ (nm), excitation energies (eV), oscillator strengths (f) of 2,4'-DBrA for gas phase, in ethanol and water solutions

TD-DFT				
	f	Major contributes	λ (nm)	E (eV)
Gas	0.2261	H-4→L+1 (53%), H→L+5 (30%)	191.02	6.4914
	0.0804	H→L+1 (67%), H-4→L (23%)	220.05	5.6351
	0.2970	H→L (79%), H-2→L (18%),	272.41	4.5520
Ethanol	0.3474	H→L+5 (73%), H-1→L+1 (13%)	182.53	6.7935
	0.1754	H-3→L+1 (56%), H-1→L+1 (36%)	194.65	6.3705
	0.0998	H→L+1 (76%), H-1→L (14%)	219.74	5.6431
	0.4917	H→L (96%)	275.28	4.5045
Water	0.3501	H→L+5 (73%), H-1→L+1 (13%)	182.41	6.7977
	0.2096	H-3→L+1 (48%), H-1→L+1 (43%)	194.25	6.3837
	0.0972	H→L+1 (76%), H-1→L (14%)	219.54	5.6481
	0.4872	H→L (96%)	275.11	4.5073

H:HOMO, L:LUMO

Primary frontier molecular orbitals (FMOs) such as, the highest occupied (HOMO) and the lowest unoccupied (LUMO) molecular orbitals supply very important information about electric and optical properties. The ability of electron giving and accepting is characterized with the HOMO and LUMO, respectively. The energy differences between HOMO-LUMO, named energy gap, are described as a potential energy, that is how much energy has to be fed into the molecule to kick it from the ground state into an excited state [62]. In the present case, energy gaps of frontier orbitals with the surfaces, activated role for excitation were pictured in Figure 9 and listed in Table 6. The energy gaps for all solvents were calculated as 4.94, 4.92 and 4.92 eV, respectively. The nodes red and green color is positive and negative on the FMOs. The charge density of HOMO localized all area outside C₁₃, C₁₄ and H atoms. The charge distribution of LUMO is changed on Br₁₇ C₁₃, C₁₄ and some H atoms. The other important energy gaps of FMOs such as, H-1→L, H→L+1, H-3→L+1 and H→L+5 (also the others) were a critical parameter in determining molecular electrical transport properties (see Table 6) given also ethanol and water solvents. Molecular orbital diagrams were listed to see energy levels, in Figure 10.

To see chemical stability, chemical hardness, electronegativity, chemical potential and electrophilicity index are good indicators for molecular systems, Parr and Pearson [63] determined chemical hardness (η) and chemical potential (μ), by $\eta=(I-H)/2$ and $\mu=-(I+H)/2$ where I and H are ionization potential and electron affinity. They are an index of reactivity and measure the escaping tendency of electron cloud, respectively. According to the chemical hardness molecules are divided into hard or soft magnitude of the energy gaps, large or small, respectively. Also hard molecules have less polarizability than the soft molecules, due to the needing big excitation energies. Electronegativity (χ) is determined as negative of the electronic chemical potential. Global electrophilicity index (ω), which measures the stabilization energy, are expressed, $\omega=\mu^2/2\eta$, in terms of electronic chemical potential μ and the chemical hardness η [64]. In the present case, chemical hardness η are nearly same magnitude for all solvents and can be say low, so the molecule no hard one. The electronegativity, chemical potential and electrophilicity index are decrease in the solvents (see Table 6).

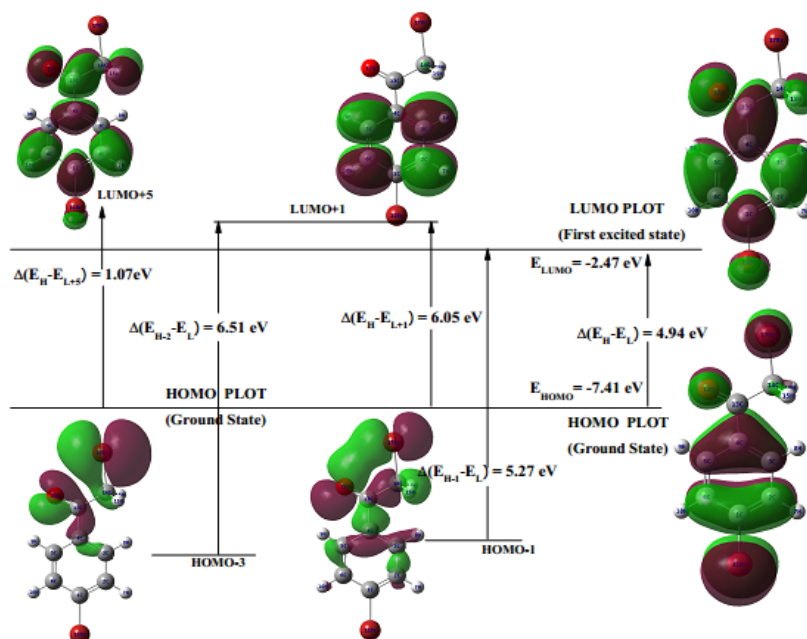


Figure 9. The selected frontier molecular orbitals of 2,4'-DBrA molecule with energy gaps

Table 6. The calculated energies values of 2,4'-DBrA molecule using B3LYP 6-311++G(d,p) basis set

TD-DFT/B3LYP/6-311++G(d,p)	Gas	Ethanol	Water
E_{total} (Hartree)			
$E_{\text{HOMO-4}}$ (eV)	-8.04	-8.05	-8.06
$E_{\text{HOMO-3}}$ (eV)	-7.87	-8.02	-8.03
$E_{\text{HOMO-2}}$ (eV)	-7.86	-7.82	-7.82
$E_{\text{HOMO-1}}$ (eV)	-7.74	-7.78	-7.77
E_{HOMO} (eV)	-7.41	-7.27	-7.27
E_{LUMO} (eV)	-2.47	-2.35	-2.35
$E_{\text{LUMO+1}}$ (eV)	-1.36	-1.10	-1.10
$E_{\text{LUMO+5}}$ (eV)	-8.48	-8.36	-8.36
$E_{\text{HOMO-4-LUMO+1}}$ gap (eV)	6.68	6.95	6.96
$E_{\text{HOMO-3-LUMO+1}}$ gap (eV)	6.51	6.92	6.93
$E_{\text{HOMO-4-LUMO}}$ gap (eV)	5.57	5.70	5.71
$E_{\text{HOMO-2-LUMO}}$ gap (eV)	5.39	5.47	5.47
$E_{\text{HOMO-1-LUMO+1}}$ gap (eV)	6.38	6.68	6.67
$E_{\text{HOMO-1-LUMO}}$ gap (eV)	5.27	5.43	5.42
$E_{\text{HOMO-LUMO}}$ gap (eV)	4.94	4.92	4.92
$E_{\text{HOMO-LUMO+1}}$ gap (eV)	6.05	6.17	6.17
$E_{\text{HOMO-LUMO+5}}$ gap (eV)	-1.07	-1.09	-1.09
Chemical hardness (η)	2.47	2.46	2.46
Electronegativity (χ)	4.94	4.81	4.81
Chemical potential (μ)	-4.94	-4.81	-4.81
Electrophilicity index (ω)	4.94	4.70	4.70

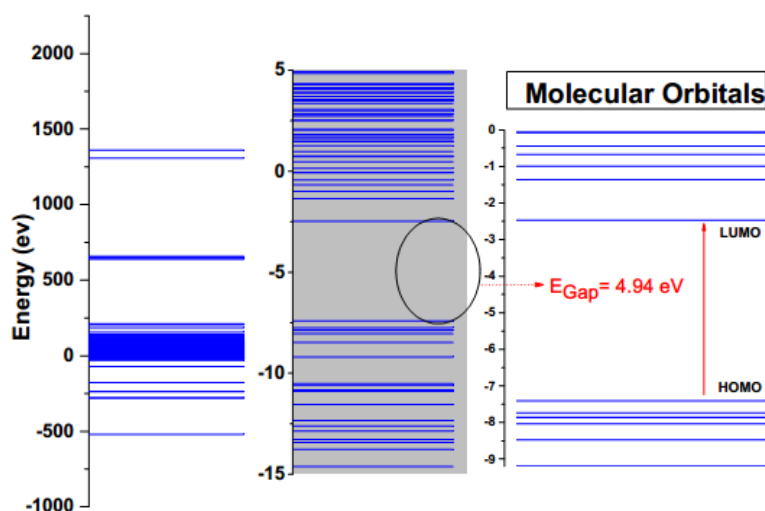


Figure 10. The molecular orbital orient of the 2,4'-DBrA molecule with energy levels

3.5.2. Total, partial, and overlap population density-of-states

The TDOS, PDOS, and OPDOS or COOP (Crystal Orbital Overlap Population)) graphics [65–67], were utilized by GaussSum 2.2 program [41] (convoluting the molecular orbital information with Gaussian curves of unit height) and full width at half maximum (FWHM) of 0.3 eV. The DOS figures specify the number of states in unit energy interval, and the concept of DOS is somewhat questionable in isolated systems. When the separated energy levels are broadened to curves artificially, DOS becomes a valuable tool for visually characterizing orbital compositions [68–70]. The interaction of HOMO and LUMO (not yield a realistic description) orbitals, in the atoms or groups described as bonding, anti-bonding and nonbonding according to OPDOS (COOP) diagrams, defined in that the positive, negative and zero values [71]. Additionally, OPDOS (COOP) diagrams used to determined and compared of the donor–acceptor properties of the molecules.

The DOS graphics are given in Figures 11–13, named TDOS, PDOS and OPDOS, respectively. To show fragment contributing to the molecular orbitals, PDOS graphic were plotted according to the fragment a phenyl ring, para bromine atom, and COCH₂Br group. The contribution of all fragment spread nearly 100 %, as phenyl ring (55%), para bromine atom (35%), COCH₂Br group (10%), in HOMO orbital. There is seen a different contribution in LUMO orbital as phenyl ring (54%), para bromine atom (3%), COCH₂Br group (43%), respectively. Easily showed in the OPDOS diagram that there is interaction or no interaction between separated groups (fragments) based on energy values of its orbitals. Such as phenyl ring ↔ COCH₂Br group, para-Br atom, (black, and blue line) system are negative (bonding interaction) in HOMO orbital of molecule. The COCH₂Br group ↔ para-Br atom is nearly zero (nonbonding interaction) in HOMO, While all of them are negative (bonding interaction) in LUMO.

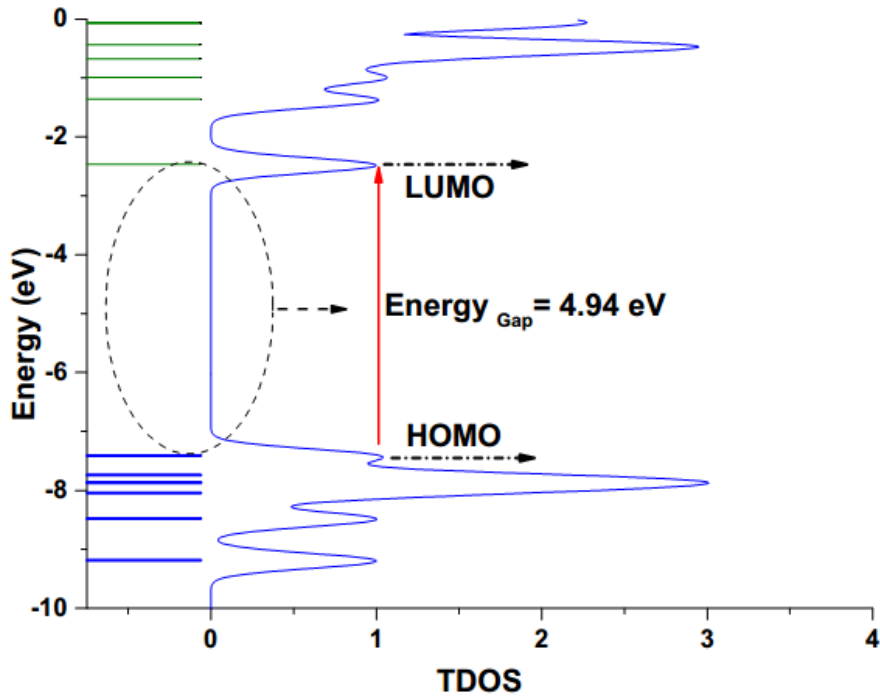


Figure 11. The total electronic density of states (TDOS) diagram of 2,4'-DBrA molecule

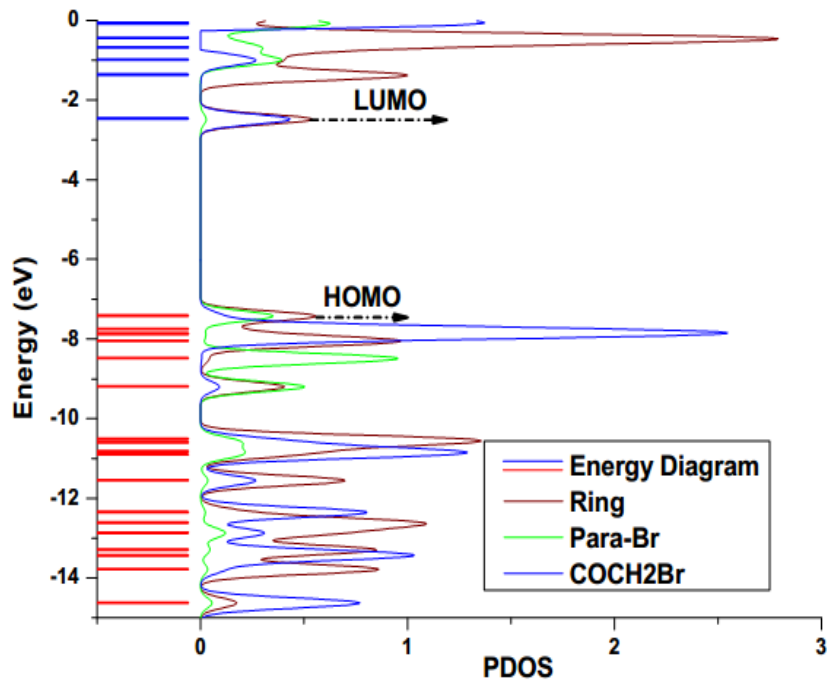


Figure 12. The partial electronic density of states (PDOS) diagram of 2,4'-DBrA molecule

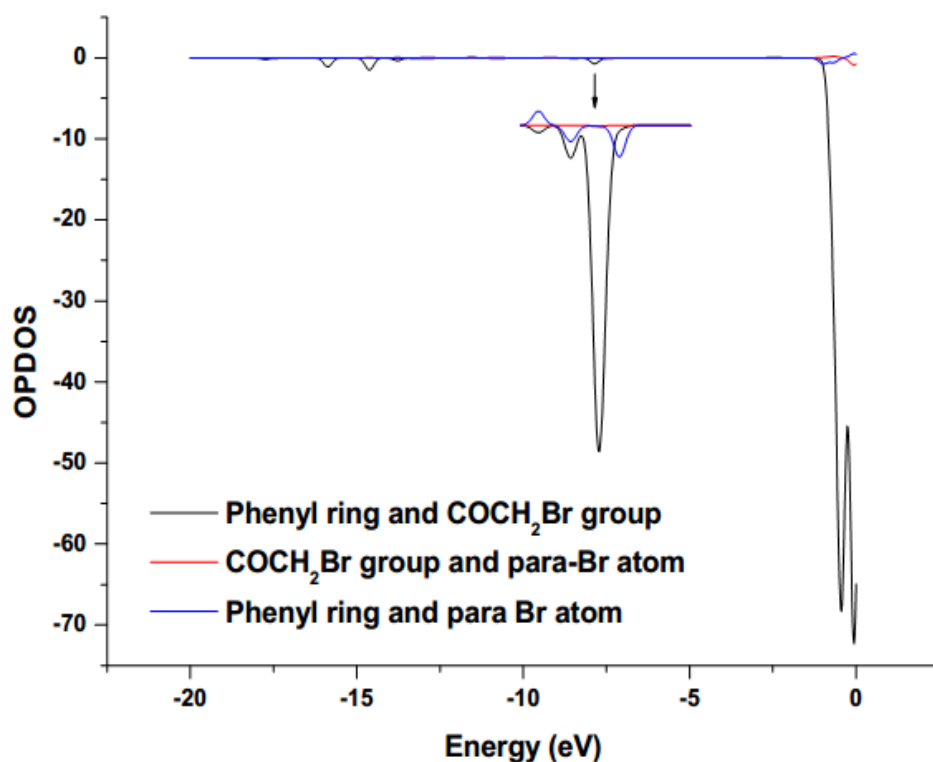


Figure 13. The overlap population electronic density of states OPDOS diagram of 2,4'-DBrA molecule

3.5.3. Molecular electrostatic potential surface

The molecular electrostatic potential surfaces (MEPs) were related to electron density, and mainly allowed to know the reactive behavior of the molecules. The positive and negative indicated that nucleophilic areas whereas, electrophilic areas, colored as blue and red, respectively [62,72,73]. Two and three dimensional (2D and 3D) MEPs diagrams were represented in Figure 14. The potential values on surfaces decrease from blue to red color and line up between $-5.083e^{-2}$ to $5.083e^{-2}$ (a.u.). The surface of MEP indicated that while regions having the negative potential are over the electronegative Br atoms and O atom, positive ones are over the hydrogen atoms especially near the CH₂ group (see Figure 14). The maximum values negative (near the O atom) and positive potential (H atoms of CH₂ group) corresponding to the electron rich and electron deficient surfaces, respectively. The MEPs enable to show the charge distributions, related properties of the title molecule.

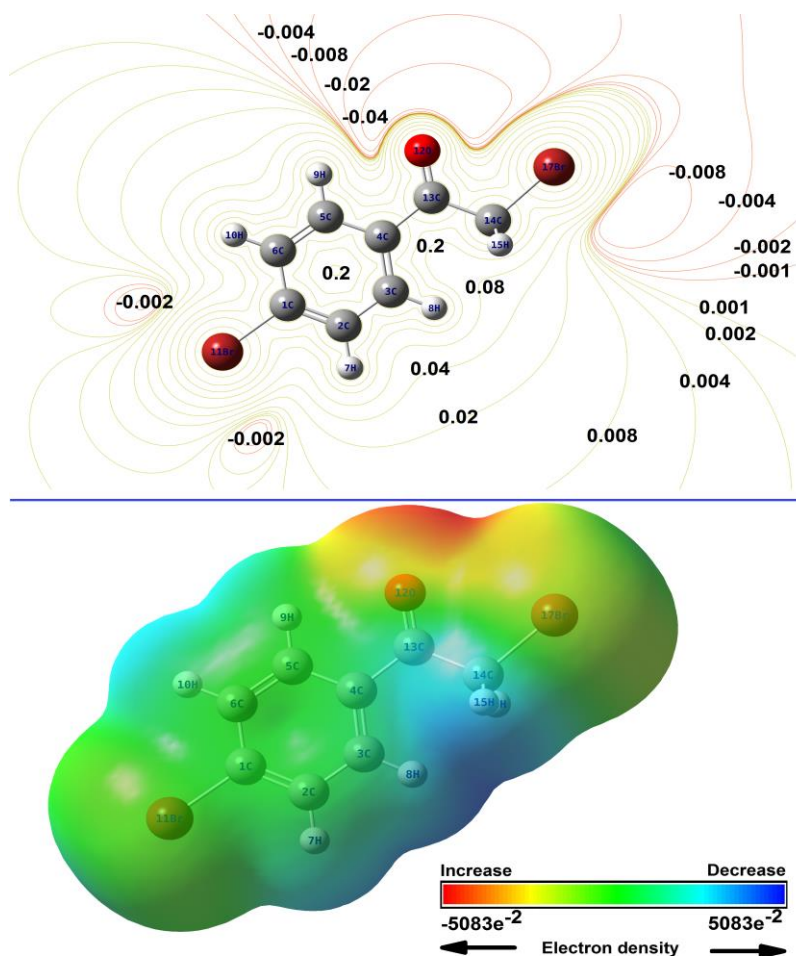


Figure 14. The molecular electrostatic potential (MEPs) surface graph for 2,4'-DBrA molecule

3.5.4. Mulliken atomic charges

Atomic charges have substantial role in application of quantum mechanical calculations of the molecular system. So, to have Mulliken atomic charges and provide a means of estimating partial atomic charges Mulliken population analysis [74] were presented for this section. The Mulliken atomic charges of acetophenone and 2,4'-DBrA molecules were obtained DFT/B3LYP method 6-31G(d) basis set, due to have the more reliable results than 6-311++G(d,p) basis set. The (6-311++G(d,p) basis set are not preferred for these reason. The atomic charges results collected Table 7 and showed in Figure 15.

To see the effect of the halogen Br atom, the acetophenone molecule was chosen for compare. The charges of the atoms were not change without carbon atom, attached Br atom in para position in the present molecule according to acetophenone molecule. So, Br atom leads to a redistribution of electron density of the aromatic carbon atom. The C₁₄ atom has same sign charges but the magnitude of charges are changed the effect of the Br₁₇ atom. (see Figure 15). The all hydrogen atoms have a positive charge, which is an acceptor, while two ones replacing the atom Br atoms have negative charges. As a results the halogen Br atom were effected the atomic charges.

Table 7. Comparison of Mulliken charges of with acetophenone and 2,4'-DBrA molecules using by B3LYP/6-31G(d) basis set

Atoms	Acetophenone	2,4'-DBrA
C1	-0.120	0.090
C2	-0.132	-0.151
C3	-0.182	-0.183
C4	0.077	0.083
C5	-0.159	-0.153
C6	-0.131	-0.149
H7	0.136	0.164
H8	0.135	0.146
H9	0.165	0.180
H10	0.139	0.166
H/Br11	0.138	-0.107
O12	-0.452	-0.429
C13	0.408	0.415
C14	-0.543	-0.406
H15	0.171	0.211
H16	0.171	0.211
H/Br17	0.182	-0.089

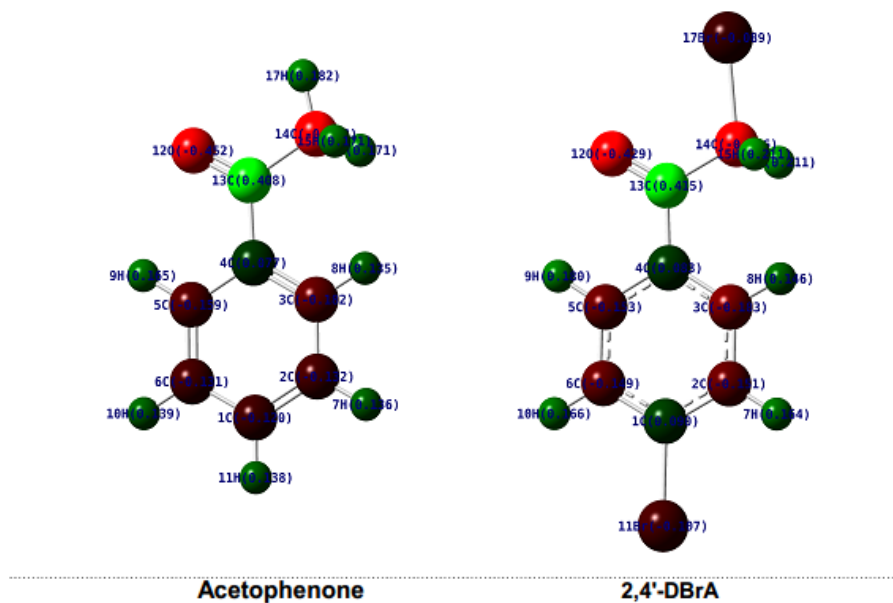


Figure 15. The Mulliken charge distribution for acetophenone and 2,4'-DBrA molecule

3.6. Thermodynamic Properties

The heat capacity (C), entropy (S), and enthalpy (H) which are of considerable thermodynamic properties were analysis for the different temperature. The temperature was varied from 100 to 700 K and was done vibrational analysis. These thermodynamic functions were obtained from theoretical harmonic frequencies and offered in Table 8. The graphical representation was also given in Figure 16 to see the relationship between temperature and these thermodynamics features.

The following quadratic formulas with their fitting factors (R^2) were also showing the relationships, respectively.

$$C = 4.87610 + 0.12540T - 5.4795 \times 10^{-5} T^2 \quad (R^2 = 0.9992)$$

$$S = 62.79641 + 0.16917T - 5.6808 \times 10^{-5} T^2 \quad (R^2 = 0.9997)$$

$$\Delta H = -0.53318 + 0.01388T + 4.1611 \times 10^{-5} T^2 \quad (R^2 = 0.9998)$$

The thermodynamic results ensure useful and more information about the chemical and physical condition of the molecule.

Table 8. Thermodynamic properties at different temperatures at the B3LYP/6-311++G(d,p) level for 2,4'-DBrA molecule

T (K)	C (cal mol ⁻¹ K ⁻¹)	S (cal mol ⁻¹ K ⁻¹)	H (kcal mol ⁻¹)
100	17.700	78.328	1.414
150	22.387	87.197	2.516
200	27.215	94.865	3.854
250	32.227	101.918	5.439
298.15	37.064	108.359	7.204
300	37.248	108.601	7.276
350	42.074	115.015	9.359
400	46.562	121.196	11.677
450	50.643	127.154	14.207
500	54.305	132.892	16.933
550	57.573	138.414	19.831
600	60.485	143.724	22.883
650	63.087	148.829	26.072
700	65.418	153.738	29.386

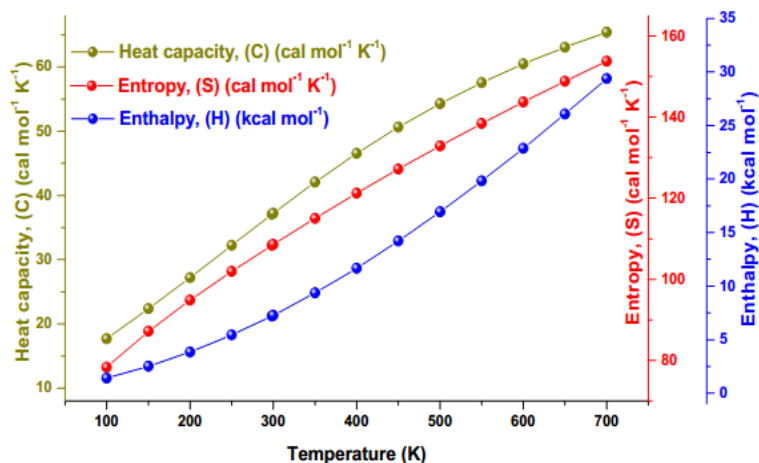


Figure 16. The correlation graphic of heat capacity, entropy, enthalpy and temperature for 2,4'-DBrA molecule

3.7. Nonlinear Optical Properties and Dipole Moment

Polarizability, anisotropy of polarizability and molecular first hyperpolarizability, which showed tensors (polarizability and hyperpolarizability) as α_{xx} , α_{xy} , α_{yy} , α_{xz} , α_{yz} , α_{zz} and β_{xxx} , β_{xxy} , β_{xyy} , β_{yyy} , β_{xxz} ,

$\beta_{xyz}, \beta_{yyz}, \beta_{xzz}, \beta_{yzz}, \beta_{zzz}$, respectively. The aforementioned NLO functions were obtained by Gaussian output job file of frequency. The units of polarizability and hyperpolarizability (α and β) were converted into from in atomic units (a.u.) to electronic units (esu) [reminding; α ; 1 a.u. = 0.1482×10^{-24} esu, β ; 1 a.u. = 8.6393×10^{-33} esu]. The all calculations were tabulated, and listed in Table 9. The following equations expressed that the mean polarizability (α_0), anisotropy of polarizability ($\Delta\alpha$) and the average value of the first hyperpolarizability ($\langle\beta\rangle$), and total dipole moment of studied molecule, μ_0 , respectively;

$$\alpha_0 = \frac{1}{3}(\alpha_{xx} + \alpha_{yy} + \alpha_{zz}) \tag{1}$$

$$\Delta\alpha = \frac{1}{\sqrt{2}} \left[(\alpha_{xx} - \alpha_{yy})^2 + (\alpha_{yy} - \alpha_{zz})^2 + (\alpha_{zz} - \alpha_{xx})^2 + 6\alpha_{xz}^2 + 6\alpha_{xy}^2 + 6\alpha_{yz}^2 \right]^{\frac{1}{2}} \tag{2}$$

$$\langle\beta\rangle = \left[(\beta_{xxx} + \beta_{yyy} + \beta_{zzz})^2 + (\beta_{yyy} + \beta_{yzz} + \beta_{yxx})^2 + (\beta_{zzz} + \beta_{zxx} + \beta_{zyy})^2 \right]^{\frac{1}{2}} \tag{3}$$

$$\mu_0 = (\mu_x^2 + \mu_y^2 + \mu_z^2)^{\frac{1}{2}} \tag{4}$$

If the molecules have relatively homogeneous charge distributions, their dipole moment are small. For NLO properties, the magnitudes of NLO functions above were important and well known for more active to be higher values. μ_0 is calculated as 3.30536 Debye (D). The components; μ_x is smallest while μ_y is highest one, and μ_z is zero. So, polarizability of the title molecule can be considered high as 14.7910×10^{-24} esu. The anisotropy of polarizability ($\Delta\alpha$), is also given end of Table 9. The first hyperpolarizability ($\langle\beta\rangle$), was predicted as obtained $9722.2965 \times 10^{-33}$ esu. These value is 12.5 times bigger than urea value ($780.323956 \times 10^{-33}$), α value is 2.9 times larger than urea (5.047709315), $\Delta\alpha$ value is 6.5 times larger than urea data (9.868773467), and μ_0 value is 2.2 times larger than those of urea (1.525686),, known experimental value polar molecule urea.

Table 9. The dipole moments μ (D), the polarizability α (a.u.), the average polarizability α_0 ($\times 10^{-24}$ esu), the anisotropy of the polarizability $\Delta\alpha$ ($\times 10^{-24}$ esu), and the first hyperpolarizability β ($\times 10^{-33}$ esu) of 2,4'-DBrA

Parameters		Parameters	
μ_x	-0.7302	β_{xxx}	-10188.1185
μ_y	-3.2237	β_{xxy}	-1116.0096
μ_z	0	β_{xyy}	312.2709
μ_0	3.30536	β_{yyy}	788.2583
α_{xx}	32.8182	β_{xxz}	0.0000
α_{xy}	0.9752	β_{xyz}	0.0000
α_{yy}	18.0429	β_{yyz}	0.0000
α_{xz}	0.0000	β_{xzz}	154.2856
α_{yz}	0.0000	β_{yzz}	208.2466
α_{zz}	11.5549	β_{zzz}	0.0000
α_0	14.7910	β_x	-9721.5621
$\Delta\alpha$	63.7373	β_y	-119.5048
		β_z	0.0000
		β	9722.2965

4. CONCLUSIONS

The study contained an experimental (FT-IR, NMR) and theoretical (DFT) calculations on the 2,4'-DBrA molecule. The title molecule was fully optimized to determine stable structure and have geometric parameters, by using B3LYP/6-311++G(d,p) level of theory. The obtained optimize results were compared X-ray results of architecture of α -bromoacetophenone and similar structures. There is a not seen big difference in theory from the experimental values. Apparent differences were evaluated in the text. Next, vibrational frequencies analyses were prepared by obtained experimental (IR) and theoretical method. The fundamental vibrational modes were assigned, based on their PED, and compared in literature values for the similar structures. The ^1H and ^{13}C NMR spectra were obtained theoretically and compared with their experimental results. Theoretical results were agreeing well correlations with their tentative NMR data. The UV-Vis calculations were prepared for gas phase and ethanol, water solvent. The FMOs, density of states (DOS), MEPs and Mulliken charges were also carried out. The Br atom play active role for the charges and electron density. Thermodynamic properties were showed that increasing with temperature, changing 50 K temperature from 100 K to 700 K. NLO properties were calculated and compared with urea results. The molecule showed that polarity and NLO active according to urea. Eventually, the obtained results were evaluated and were showing very well correlations and agreement in obtained experimental results and in the literature.

REFERENCES

- [1] Griffin, R.N., Phosphorescence of Aromatic Ketones in Low-Temperature Glasses, Photochemistry and Photobiology. (1968) 7 159–173.
- [2] Lutz, H., Duval, M.C., Breheret, E., Lindqvist, L., Solvent effects on acetophenone photoreduction studied by laser photolysis, The Journal of Physical Chemistry. (1972) 76 821–822.
- [3] Scharf, G., Winefordner, J.D., Phosphorescence characteristics of acetophenone, benzophenone, p-aminobenzophenone and michlercs ketone in various environments, Talanta. (1986) 33 17–25.
- [4] Proksch, P., Rodriguez, E., Chromenes and benzofurans of the asteraceae, their chemistry and biological significance, Phytochemistry. (1983) 22 2335–2348.
- [5] Tomás-Barberán, F., Iniesta-Sanmartín, E., Tomás-Lorente, F., Rumero, A., Antimicrobial phenolic compounds from three Spanish Helichrysum species, Phytochemistry. (1990) 29 1093–1095.
- [6] Buckle, D.R., Smith, H., Cantello, B.C.C., Substituted ω -nitroacetophenones, (1976).
- [7] Buckle, D.R., Smith, H., Cantello, B.C.C., Acetophenone derivatives, (1976).
- [8] Sivakumar, P.M., Sheshayan, G., Doble, M., Experimental and QSAR of Acetophenones as Antibacterial Agents, Chemical Biology & Drug Design. (2008) 72 303–313.
- [9] Sittig, M., Pharmaceutical manufacturing encyclopedia, Noyes publ., 1988.
- [10] Amin, S.I., Walker, J.A., Process for preparing arylalkanoic acid derivatives, 1979.
- [11] Zhang, X., Shan, L., Huang, H., Yang, X., Liang, X., Xing, A., et al., Rapid identification of acetophenones in two Cynanchum species using liquid chromatography-electrospray ionization tandem mass spectrometry., Journal of Pharmaceutical and Biomedical Analysis. (2009) 49 715–725.
- [12] Liu, Z., Sun, Y., Wang, J., Zhu, H., Zhou, H., Hu, J., et al., Preparative isolation and purification of acetophenones from the Chinese medicinal plant Cynanchum bungei Decne. by high-speed counter-current chromatography, Separation and Purification Technology. (2008) 64 247–252.

- [13] Cacchi, S., Fabrizi, G., Gavazza, F., Goggiamani, A., Palladium-Catalyzed Reaction of Aryl Iodides with Acetic Anhydride. A Carbon Monoxide-Free Synthesis of Acetophenones, *Organic Letters*. (2003) 5 289–291.
- [14] Prasad, Y.R., Rao, a S., Rambabu, R., Synthesis of Some 4'-Amino Chalcones and their Antiinflammatory and Antimicrobial Activity, *Asian Journal of Chemistry*. (2009) 21 907–914.
- [15] Gupta, M.P., Prasad, S.M., The crystal structure of [alpha]-bromoacetophenone, *Acta Crystallographica Section B*. (1971) 27 1649–1653.
- [16] Baker, L.-J., Copp, B.R., and Rickard, C.E.F., 2'-Amino-5'-bromoacetophenone, *Acta Crystallographica Section E Structure Reports Online*. (2001) 57 o996–o998.
- [17] Seth, S.K., Hazra, D.K., Mukherjee, M., Kar, T., Synthesis, structural elucidation and DFT studies of ortho-hydroxy acetophenones, *Journal of Molecular Structure*. (2009) 936 277–282.
- [18] Piro, O.E., Echeverría, G.A., Lizarraga, E., Romano, E., Catalán, C.A.N., Brandán, S.A., Molecular structure of 4-hidroxy-3-(3-methyl-2-butenyl) acetophenone, a plant antifungal, by X-ray diffraction, DFT calculation, and NMR and FTIR spectroscopy., *Spectrochimica Acta. Part A, Molecular and Biomolecular Spectroscopy*. (2013) 101 196–203.
- [19] Rodríguez, A.M., Giannini, F.A., Baldoni, H.A., Santagata, L.N., Zamora, M.A., Zacchino, S., et al., Conformational potential energy curves of acetophenone and α -substituted acetophenones, *Journal of Molecular Structure: THEOCHEM*. (1999) 463 271–281.
- [20] Xiao, H.-Y., Liu, Y.-J., Fang, W.-H., Density functional theory investigation of the photodissociation channels of acetophenone, *Journal of Molecular Structure: THEOCHEM*. (2007) 802 99–103.
- [21] Krishnakumar, V., Balachandran, V., DFT studies, vibrational spectra and conformational stability of 4-hydroxy-3-methylacetophenone and 4-hydroxy-3-methoxyacetophenone., *Spectrochimica Acta. Part A, Molecular and Biomolecular Spectroscopy*. (2005) 61 2510–2525.
- [22] Anbusrinivasan, P., Kavitha, S., Growth and characterization studies of 2-bromo-4-chloroacetophenone crystals, *Asian Journal of Chemistry*. (2008) 20 979–982.
- [23] Anbarasu, P., Arivazhaganb, M., Scaled quantum chemical study of structure and vibrational spectra of 5-fluro-2-hydroxyacetophenone, *Indian Journal of Pure and Applied Physics*. (2011) 49 227–233.
- [24] Udhayakala, P., Rajendiran, T. V, Seshadri, S., Gunasekaran, S., Quantum chemical vibrational study, molecular property and HOMO-LUMO energies of 3-bromoacetophenone for Pharmaceutical application, *Journal of Chemical and Pharmaceutical Research*. (2011) 3 610–625.
- [25] Subramanian, M.K., Anbarasan, P.M., Ilangovan, V., Babu, S.M., FT-IR, NIR-FT-Raman and gas phase infrared spectra of 3-aminoacetophenone by density functional theory and ab initio Hartree-Fock calculations, *Spectrochimica Acta - Part A: Molecular and Biomolecular Spectroscopy*. (2008) 71 59–67.
- [26] Ramalingam, S., Anbusrinivasan, P., Periandy, S., FT-IR and FT-Raman spectral investigation, computed IR intensity and Raman activity analysis and frequency estimation analysis on 4-chloro-2-bromoacetophenone using HF and DFT calculations., *Spectrochimica Acta. Part A, Molecular and Biomolecular Spectroscopy*. (2011) 78 826–834.

- [27] Jeyavijayan, S., Molecular structure, spectroscopic (FTIR, FT-Raman, ^{13}C and ^1H NMR, UV), polarizability and first-order hyperpolarizability, HOMO-LUMO analysis of 2,4-difluoroacetophenone., *Spectrochimica Acta. Part A, Molecular and Biomolecular Spectroscopy.* (2015) 136 B 553–566.
- [28] Parimala, K., Balachandran, V., Structural study, NCA, FT-IR, FT-Raman spectral investigations, NBO analysis and thermodynamic properties of 2',4'-difluoroacetophenone by HF and DFT calculations., *Spectrochimica Acta. Part A, Molecular and Biomolecular Spectroscopy.* (2013) 110 269–284.
- [29] SDBS Web: <http://sdb.srioddb.aist.go.jp> (National Institute of Advanced Industrial Science and Technology), SDBS Web: <http://sdb.srioddb.aist.go.jp> (National Institute of Advanced Industrial Science and Technology), (2016).
- [30] Frisch, M.J., Trucks, G.W., Schlegel, H.B., Scuseria, G.E., Robb, M.A., Cheeseman, J.R., et al., *Gaussian 09*, Gaussian, Inc., Wallingford, CT. (2009).
- [31] Hohenberg, P., Kohn, W., Inhomogeneous Electron Gas, *Physical Review.* (1964) 136 B864–B871.
- [32] Becke, A.D., Density-functional thermochemistry. III. The role of exact exchange, *The Journal of Chemical Physics.* (1993) 98 5648–5652.
- [33] Becke, A.D., Density-functional exchange-energy approximation with correct asymptotic behavior, *Physical Review A.* (1988) 38 3098–3100.
- [34] Lee, C., Yang, W., Parr, R.G., Development of the Colle-Salvetti correlation-energy formula into a functional of the electron density, *Physical Review B.* (1988) 37 785–789.
- [35] Jamróz, M.H., Vibrational energy distribution analysis (VEDA): scopes and limitations., *Spectrochimica Acta Part A: Molecular and Biomolecular Spectroscopy.* (2013) 114 220–230.
- [36] Dennington, R., Keith, T., Millam, J., *GaussView*, version 5, 2009.
- [37] Guillaumont, D., Nakamura, S., Calculation of the absorption wavelength of dyes using time-dependent density-functional theory (TD-DFT), *Dyes and Pigments.* (2000) 46 85–92.
- [38] Fabian, J., TDDFT-calculations of Vis/NIR absorbing compounds, *Dyes and Pigments.* (2010) 84 36–53.
- [39] Ditchfield, R., Molecular Orbital Theory of Magnetic Shielding and Magnetic Susceptibility, *The Journal of Chemical Physics.* (1972) 56 5688–5691.
- [40] Wolinski, K., Hinton, J.F., Pulay, P., Efficient implementation of the gauge-independent atomic orbital method for NMR chemical shift calculations, *Journal of the American Chemical Society.* (1990) 112 8251–8260.
- [41] O'boyle, N.M., Tenderholt, A.L., Langner, K.M., Software News and Updates cclib: A Library for Package-Independent Computational Chemistry Algorithms, *Journal of Computational Chemistry.* (2008) 29 839–845.
- [42] Karabacak, M., Kurt, M., The spectroscopic (FT-IR and FT-Raman) and theoretical studies of 5-bromo-salicylic acid, *Journal of Molecular Structure.* (2009) 919 215–222.

- [43] Karabacak, M., Kose, E., Atac, A., Sas, E.B., Asiri, A.M., Kurt, M., Experimental (FT-IR, FT-Raman, UV-Vis, ¹H and ¹³CNMR) and computational (density functional theory) studies on 3-bromophenylboronic acid, *Journal of Molecular Structure*. (2014) 1076 358–372.
- [44] Karabacak, M., Cinar, M., Ermec, S., Kurt, M., Experimental vibrational spectra (Raman, infrared) and DFT calculations on monomeric and dimeric structures of 2- and 6-bromonicotinic acid, *Journal of Raman Spectroscopy*. (2010) 41 98–105.
- [45] Dollish, F.R., Fateley, W.G., Bentley, F.F., *Characteristic Raman frequencies of organic compounds*, Wiley, 1974.
- [46] Colthup, N.B., Daly, L.H., Wiberley, S.E., *Introduction to Infrared and Raman Spectroscopy*, Academic Press, 1990.
- [47] Varsányi, G., *Assignments for vibrational spectra of seven hundred benzene derivatives*, Halsted Press, 1974.
- [48] Mooney, E.F., *The infrared spectra of chloro- and bromobenzene derivatives—I*, *Spectrochimica Acta*. (1963) 19 877–887.
- [49] Sas, E.B., Kose, E., Kurt, M., Karabacak, M., FT-IR, FT-Raman, NMR and UV-Vis spectra and DFT calculations of 5-bromo-2-ethoxyphenylboronic acid (monomer and dimer structures), *Spectrochimica Acta Part A: Molecular and Biomolecular Spectroscopy*. (2015) 137C 1315–1333.
- [50] Sundaraganesan, N., Meganathan, C., Anand, B., Lapouge, C., FT-IR, FT-Raman spectra and ab initio DFT vibrational analysis of p-bromophenoxyacetic acid., *Spectrochimica Acta Part A: Molecular and Biomolecular Spectroscopy*. (2007) 66 773–780.
- [51] Kurt, M., DFT simulations and Vibrational spectra of 4-chloro and 4-bromophenylboronic acid molecules, *Journal of Raman Spectroscopy*. (2009) 40 67–75.
- [52] Smith, B., *Infrared spectral interpretation: a systematic approach*, 1998. (accessed June 6, 2014).
- [53] Socrates, G., *Infrared and Raman Characteristic Group Frequencies: Tables and Charts*, John Wiley & Sons Ltd., West Sussex, England, 2001.
- [54] Silverstein, R.M., Webster, F.X., Kiemle, D.J., *Spectrometric identification of organic compounds*, John Wiley & Sons, 2005.
- [55] Gianturco, M.A., Pitcher, R.G., *New Spectra-Structure Correlations of Aliphatic Ketones*, *Applied Spectroscopy*. (1965) 19 109–110.
- [56] Schlick, T., *Molecular Modeling and Simulation: An Interdisciplinary Guide: An Interdisciplinary Guide*, 2nd ed., Springer, Newyork, USA, 2010.
- [57] Subramanian, N., Sundaraganesan, N., Jayabharathi, J., Molecular structure, spectroscopic (FT-IR, FT-Raman, NMR, UV) studies and first-order molecular hyperpolarizabilities of 1,2-bis(3-methoxy-4-hydroxybenzylidene)hydrazine by density functional method., *Spectrochimica Acta Part A: Molecular and Biomolecular Spectroscopy*. (2010) 76 259–269.
- [58] Karabacak, M., Karaca, C., Atac, A., Eskici, M., Karanfil, A., Kose, E., Synthesis, analysis of spectroscopic and nonlinear optical properties of the novel compound: (S)-N-benzyl-1-phenyl-5-(thiophen-3-yl)-4-pentyn-2-amine., *Spectrochimica Acta Part A: Molecular and Biomolecular Spectroscopy*. (2012) 97 556–567.

- [59] Kalinowski, H.O., Berger, S., Braun, S., Carbon-13 NMR spectroscopy, 1988.
- [60] Pihlaja, K., Kleinpeter, E., Carbon-13 NMR Chemical Shifts in Structural and Stereochemical Analysis, VCH, 1994.
- [61] Breitmaier, E., Voelter, W., Carbon-13 NMR spectroscopy, Carbon 13 NMR Spectroscopy. (1987).
- [62] Arivazhagan, M., Anitha Rexalin, D., FT-IR, FT-Raman, NMR studies and ab initio-HF, DFT-B3LYP vibrational analysis of 4-chloro-2-fluoroaniline., Spectrochimica Acta Part A: Molecular and Biomolecular Spectroscopy. (2012) 96 668–676.
- [63] Parr, R.G., Pearson, R.G., Absolute hardness: companion parameter to absolute electronegativity, Journal of the American Chemical Society. (1983) 105 7512–7516.
- [64] Parr, R.G., Yang, W., Density-Functional Theory of Atoms and Molecules, Oxford University Press, USA, 1989.
- [65] Hoffman, R., Solids and surfaces: a chemist's view of bonding in extended structures, 1988.
- [66] Highbanks, T., Hoffmann, R., Chains of trans-edge-sharing molybdenum octahedra: metal-metal bonding in extended systems, Journal of the American Chemical Society. (1983) 105 3528–3537.
- [67] Małecki, J.G., Synthesis, crystal, molecular and electronic structures of thiocyanate ruthenium complexes with pyridine and its derivatives as ligands, Polyhedron. (2010) 29 1973–1979.
- [68] Gorelsky, S.I., Ghosh, S., Solomon, E.I., Mechanism of N₂O Reduction by the μ -4-S Tetranuclear Cu₂Z Cluster of Nitrous Oxide Reductase, Journal of the American Chemical Society. (2005) 128 278–290.
- [69] Ghosh, S., Gorelsky, S.I., Chen, P., Cabrito, I., Moura, J.J.G., Moura, I., et al., Activation of N₂O reduction by the fully reduced micro4-sulfide bridged tetranuclear Cu Z cluster in nitrous oxide reductase., Journal of the American Chemical Society. (2003) 125 15708–15709.
- [70] Platas-Iglesias, C., Esteban-Gómez, D., Enríquez-Pérez, T., Avecilla, F., de Blas, A., Rodríguez-Blas, T., Lead(II) Thiocyanate Complexes with Bibracchial Lariat Ethers: An X-ray and DFT Study, Inorganic Chemistry. (2005) 44 2224–2233.
- [71] Chen, M., Waghmare, U. V., Friend, C.M., Kaxiras, E., A density functional study of clean and hydrogen-covered α -MoO₃(010): Electronic structure and surface relaxation, The Journal of Chemical Physics. (1998) 109 6854–6860.
- [72] Okulik, N., Jubert, A.H., Theoretical analysis of the reactive sites of non-steroidal anti-inflammatory drugs, Internet Electronic Journal of Molecular Design. (2005) 4 17–30.
- [73] Luque, F.J., López, J.M., Orozco, M., Perspective on “Electrostatic interactions of a solute with a continuum. A direct utilization of ab initio molecular potentials for the prevision of solvent effects,” Theoretical Chemistry Accounts: Theory, Computation, and Modeling (Theoretica Chimica Acta). (2000) 103 343–345.
- [74] Mulliken, R.S., Electronic Population Analysis on LCAO-MO Molecular Wave Functions. I, The Journal of Chemical Physics. (1955) 23 1833–1840.